Acta Geochim (2017) 36(1):52–65
DOI 10.1007/s11631-016-0120-8

ORIGINAL ARTICLE

Platinum-group element geochemistry of mafic rocks from the Dongchuan area, southwestern China

Siqi Yang[1,2] · Hong Zhong[1] · Weiguang Zhu[1] · Wenjun Hu[1] · Zhongjie Bai[1]

Received: 26 April 2016 / Revised: 8 July 2016 / Accepted: 15 August 2016 / Published online: 2 September 2016

Abstract Mafic intrusions and dykes are well preserved in the Yinmin and Lanniping districts, located within the western margin of the Yangtze Block, SW China. Although these mafic rocks from the two areas formed during different periods, they share similar ranges of PGE concentration. Most of the Yinmin gabbroic dykes contain relatively high PGE concentrations (PGEs = 13.9–87.0 ppb) and low S contents (0.003 %–0.020 %), higher than the maximum PGE concentrations of mafic magmas melting from the mantle. Two exceptional Yinmin samples are characterized by relatively low PGE (PGEs = 0.31–0.37 ppb) and high S (0.114 %–0.257 %) contents. In contrast, most samples from the Lanniping gabbroic intrusion have low PGE concentrations (PGEs = 0.12–1.02 ppb) and high S contents (0.130 %–0.360 %), except that the three samples exhibit relatively high PGE (PGEs = 16.3–34.8 ppb) and low S concentrations (0.014 %–0.070 %). All the Yinmin and Lanniping samples are characterized by the enrichment of PPGE relative to IPGE in the primitive-mantle normalized diagrams, and the high-PGE samples exhibit obvious Ru anomalies. This study suggests that during the ascent of the parental magma, removal of Os–Ir–Ru alloys and/or chromite/spinel leads to high Pd/Ir ratios and Ru anomalies for the Yinmin high-PGE samples and relatively lower Pd/Ir ratios and Ru anomalies for the Lanniping low-PGE samples. We propose that the magmas parental to the Yinmin gabbroic dykes are initially S-unsaturated, and subsequently, minor evolved magma reached sulfur saturation and led to sulfide segregation. Although the Lanniping parental magmas are originally not saturated in S, the high Cu/Pd ratios (3.8×10^4 to 3.2×10^6) for most of the Lanniping samples indicate the S-saturated state and sulfide segregation. A calculation shows that the PGE-poor magmas might have experienced 0.01 %–0.1 % sulfide segregation in the magma chamber. Therefore, our study provides a possible opportunity to discover PGE-enriched sulfide mineralization somewhere near or within the Lanniping mafic intrusion.

Keywords Mafic intrusions and dykes · Platinum-group element · Sulfide saturation · Dongchuan area

1 Introduction

The platinum-group elements (PGE) form a coherent group of siderophile and chalcophile elements that are sensitive to reveal aspects of such processes as partial melting in the mantle, crystal fractionation and S-saturation of magmas (Barnes et al. 1993). It is well documented that S-unsaturated melts may have relatively high PGEs, especially PPGE (Pd-group PGEs, including Rh, Pt, Pd) (Keays 1995; Seitz and Keays 1997). Examples of rocks formed from such S-unsaturated magmas are komatiites, boninites and high-Mg tholeiites with high PGE contents (Hamlyn et al. 1985; Zhou 1994; Seitz and Keays 1997). S-saturated melts may have relatively low PGEs due to the high partition coefficient of PGEs between the sulfide melts and the silicate magmas.

The Dongchuan deposits have been mined and studied for several decades. However, the genesis of the Dongchuan-type copper deposits has long been debated and several

✉ Hong Zhong
zhonghong@vip.gyig.ac.cn

[1] State Key Laboratory of Ore Deposit Geochemistry, Institute of Geochemistry, Chinese Academy of Sciences, Guiyang 550081, China

[2] University of Chinese Academy of Sciences, Beijing 100049, China

genetic models have been proposed. Some researchers invoked an epigenetic model in which copper sulfides were precipitated from magmatic-hydrothermal fluids (Meng et al. 1948; Li et al. 1953). Some researchers advocated a syn-sedimentary, exhalative model based on the strata-bound nature of orebodies (Gong and Wang 1981; Gong et al. 1996). A composite diagenetic model was proposed, wherein metals were derived from continental red beds and precipitated in reduced sulfur-bearing dolostones during diagenetic or Late metamorphic events (Ran 1983; Hua 1990). Lately, these deposits were originally considered to be volcanogenic and similar to volcanogenic massive sulfide (VMS) deposits elsewhere (Qian and Shen 1990; Sun et al. 1991a, b). However, some researchers suggested that these deposits may be epithermal and linked to Neoproterozoic magmatism (Li et al. 2003a, b; Ye et al. 2004). Recent research has identified that these deposits are similar to iron oxide–copper–gold (IOCG) deposits or sedimentary rock-hosted strata-bound copper (SSC) deposits located elsewhere (Zhao et al. 2011; Hou et al. 2014).

Mineralization ages of the Cu–Fe deposits in the Dongchuan region were poorly constrained, largely due to the lack of minerals that are suitable for the isotopic dating method. Previous geochronological studies, mostly using sulfide Pb–Pb dating, yielded ages spanning from 1.7 to 0.7 Ga (e.g., Gong et al. 1996). Some researchers attempted to date the mineralization using the $^{40}Ar/^{39}Ar$ analysis of inclusion fluids extracted from quartz, yielding ages mostly between 780 and 700 Ma (Qiu et al. 2002; Ye et al. 2004). Recent research has identified that sulfide Re–Os ages thus constrain the timing of the mineralization at ~1700 Ma (Zhao et al. 2013). The mineralization age of these deposits has thus been debated. However, these deposits are generally, temporally and spatially, related to igneous intrusions and the role of magmatism in the genesis of the Dongchuan deposits needs more research.

The Dongchuan gabbroic dykes and intrusions in the western Yangtze Block are spatially related to the Cu–Fe ore deposits (Fig. 1b). Therefore, one of the points of view is that the mafic intrusions controlled the formation of these deposits from the material source and the heat source (Liu et al. 2011; Hou et al. 2015). However, the opinion needs more evidence to support it. The PGEs, in combination with Ni and Cu contents, could provide valuable information on the petrogenesis of mafic–ultramafic rocks (e.g., Lightfoot and Keays 2005; Maier 2005). Moreover, partial melting in the mantle, crystal fractionation and sulfide saturation of magmas could directly indicate the characteristic of source region and evolution of magmas. From another point of view, the relationship between the gabbroic dykes and intrusions and Cu–Fe ore deposits could be indirectly enlightened through a discussion about the PGE behaviors of the Dongchuan gabbroic intrusive rocks.

In this study, the geochemical compositions of the Yinmin gabbroic dykes and Lanniping gabbroic intrusions will be discussed and compared to each other. Some geochemical data (Gong et al. 1996; Chen 1998; Liu et al. 2011; Zhao et al. 2010, 2013) of gabbroic rocks in these areas have previously been reported, except the PGE compositions. As these gabbroic intrusive rocks may undergo the same or different evolutionary processes, it is more appropriate to discuss them separately. The PGE behaviors of the Early Proterozoic and Neoproterozoic gabbroic dykes and intrusions in Dongchuan might provide new constraints on the processes that resulted in the unique PGE features of these rocks, and thus be used to elucidate their petrogenesis and to evaluate whether they have the potential for economic PGE mineralization.

2 Geological background and petrography

The South China Block consists of two major Precambrian blocks: the Yangtze Block to the northwest and the Cathaysia Block to the southeast (present coordinates), with the Late-Mesoproterozoic to Earliest Neoproterozoic Sibao Orogen situated between them. The Kangdian area is located near the western margin of the Yangtze Block, South China (Fig. 1a). The oldest supracrustal rocks in this area are the Late Paleo- to Meso-proterozoic meta-volcanic and sedimentary rocks of the Dahongshan Group (Greentree and Li 2008), the Hekou Group (He 2009; Zhao and Zhou 2011), and the Kunyang Group (Yin et al. 2011), occurring along the Luzhijiang fault and a series of related NNE-trending faults (Fig. 1b). The Dahongshan Group is a sequence of meta-volcanic rocks, and is generally considered to be the equivalent of the Hekou Group (e.g., Zhao et al. 2010), as confirmed by the zircon U–Pb ages for meta-clastic and meta-carbonate rocks from the Hekou Group (Greentree and Li 2008; Zhao and Zhou 2011).

The Kunyang Group in the study region was divided into the Upper and Lower Kunyang groups (e.g., Zhao and Zhou 2011; Zhao et al. 2010). Zhao et al. (2010) interpreted the Lower Kunyang groups, Dahongshan groups and Hekou groups as stratigraphically correlatable units. The Lower Kunyang Group, from the base upward, includes the Yinmin, Luoxue, E'touchang, and Luzhijiang formations, whereas the Upper Kunyang Group consists of the Huangcaoling, Heishantou, Dalongkou, and Meidang formations. The Lower Kunyang Group likely formed between ~1.7 and ~1.5 Ga by the ages of detrital zircons (Sun et al. 2009; Zhao et al. 2010). Several meta-volcanic layers in the Upper Kunyang groups have zircon U–Pb ages of ~1.0 Ga (Mou et al. 2003; Greentree et al. 2006; Geng et al. 2007; Zhang et al. 2007). These rocks are overlain by a thick sequence (maximum >9 km) of Neoproterozoic

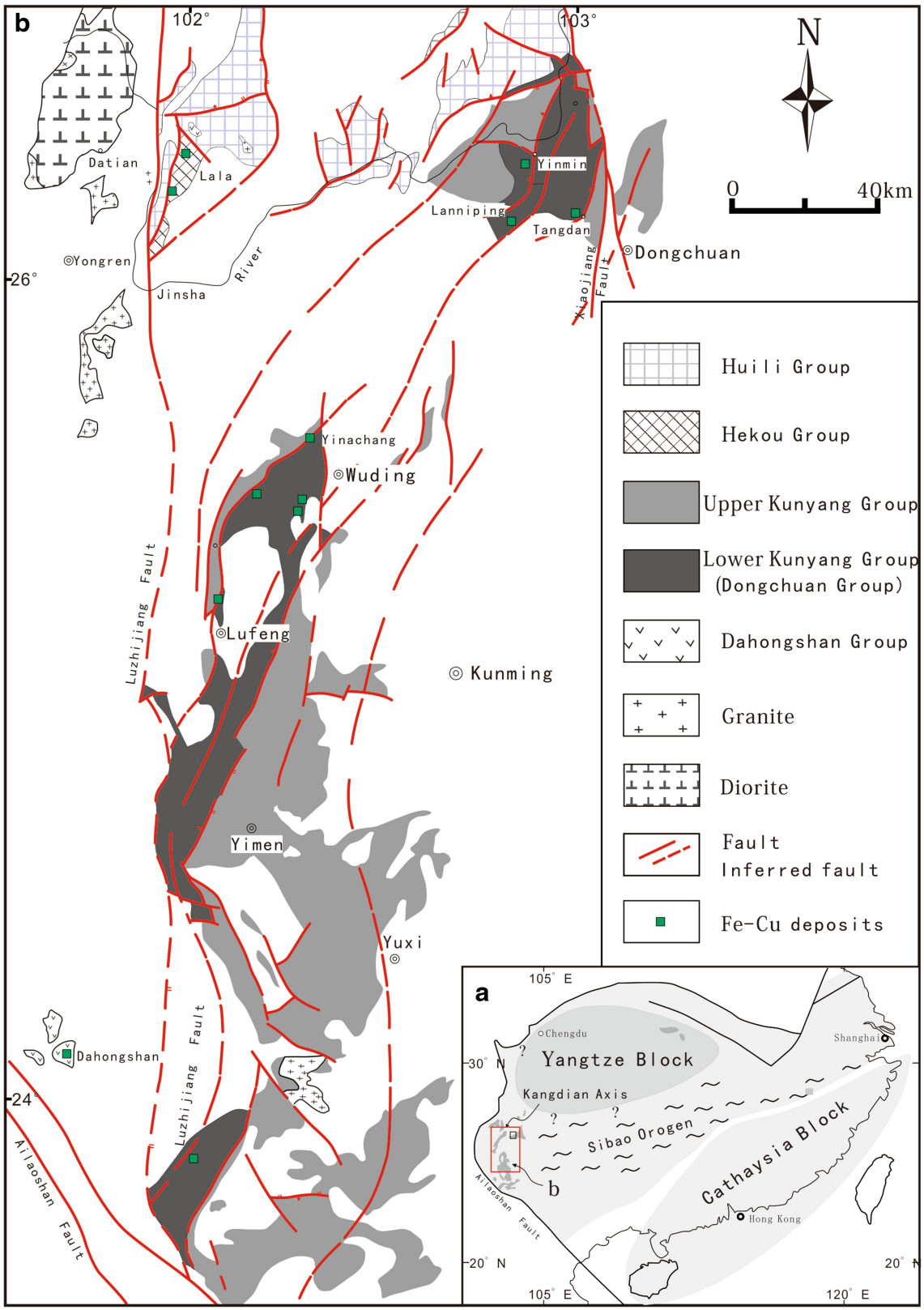

Fig. 1 **a** Simplified tectonic map showing the study area in relation to major tectonic units in South China (Li et al. 2007); **b** Geological map of Precambrian supracrustal rocks and Neoproterozoic intrusions in the Kangdian region, SW China (modified from Wu et al. 1990)

(850–540 Ma) to Permian strata composed of clastic, carbonate and volcanic rocks.

Numerous Cu–Fe deposits are hosted in the Kunyang Groups. Parts of the Cu–Fe deposits consist of the stratiform and disseminated Cu-sulfide and Fe-oxide ores in the dolostone. The other Cu–Fe deposits are hosted in metavolcanic or distributed around the dykes and intrusions. Both types of deposits were traditionally considered to be syngenetic in origin. The deposits related to igneous intrusions are mainly discussed in this paper. The Cu-sulfide ores occur as disseminations, veinlets, and to a lesser extent, stockwork structures and the sulfides are preferentially concentrated within or at the peripheries of dykes and intrusions. The Fe-oxide ores are roughly concordant and disseminated in the dykes and intrusions. From the above description, there are some relationships between the mafic intrusions and these deposits.

This paper focuses on two areas, viz., the Lanniping district and the Yinmin district in the Dongchuan area. A number of mafic intrusions, dominantly composed of gabbroic rocks, are distributed as dykes in the Yinmin area and irregular small intrusions in the Lanniping area (Fig. 2). The Yinmin and Lanniping gabbroic rocks are bounded by a series of faults in the northeast of the Dongchuan area (Fig. 1b). The distribution area of exposed Yinmin mafic dykes are up to 6 km long and commonly 9 km wide, striking NW 307°–349° and the distribution range of exposed Lanniping intrusion is relatively limited to an area of 3 km wide and 1.8 km long. The majority of gabbros are mainly hosted in the Yinmin and Luoxue Formations of the Kunyang Group. The group units cover the Early Paleoproterozoic formation of the Caiyuanwan group and are overlain by the Heishantou, Qinglongshan and Dengying Formations, from the base to the top (Fig. 2). The relationship between the succession of strata and emplacement of gabbros is also accordant with the dating results. The gabbroic intrusion in Lanniping was dated at 1088 ± 5.6 Ma (our unpublished data), obviously younger than the zircon U–Pb age of 1695 ± 16 Ma (Zhao and Zhou 2011) for the gabbroic dyke intruding the sequence in the Yinmin area.

The Yinmin Formation is mainly composed of hematite-bearing purplish-red siltstone and sandstone, with basal conglomerate in places (Wu et al. 1990). These rocks are thought to be the oldest continental red-bed units in the Yangtze Block (Hua 1990; Wu et al. 1990; Zhao et al. 2010). The uppermost part of the Yinmin Formation consists of intercalated siltstone and dolostone that are transitional to the thick-layered basal dolostone of the Luoxue Formation. Conformably overlying the Yinmin Formation, the Luoxue Formation consists of thick layers of grayish-white dolostone and argillo-arenaceous dolostone. The contact between the Yinmin and Luoxue Formations is generally the main copper-rich matrix.

Most of the dykes and intrusions consist of medium- to coarse-grained gabbroic rocks, and the sizes of the mineral grains are typically larger in the Lanniping district than the dykes in the Yinmin area. In addition, there are few sulfides (chalcopyrite, bornite and chalcocite) in the Lanniping intrusion. From microscopic studies, plagioclases range from subhedral to euhedral with small crystals, and were altered to clay or calcite. Xenomorphic granular pyroxenes

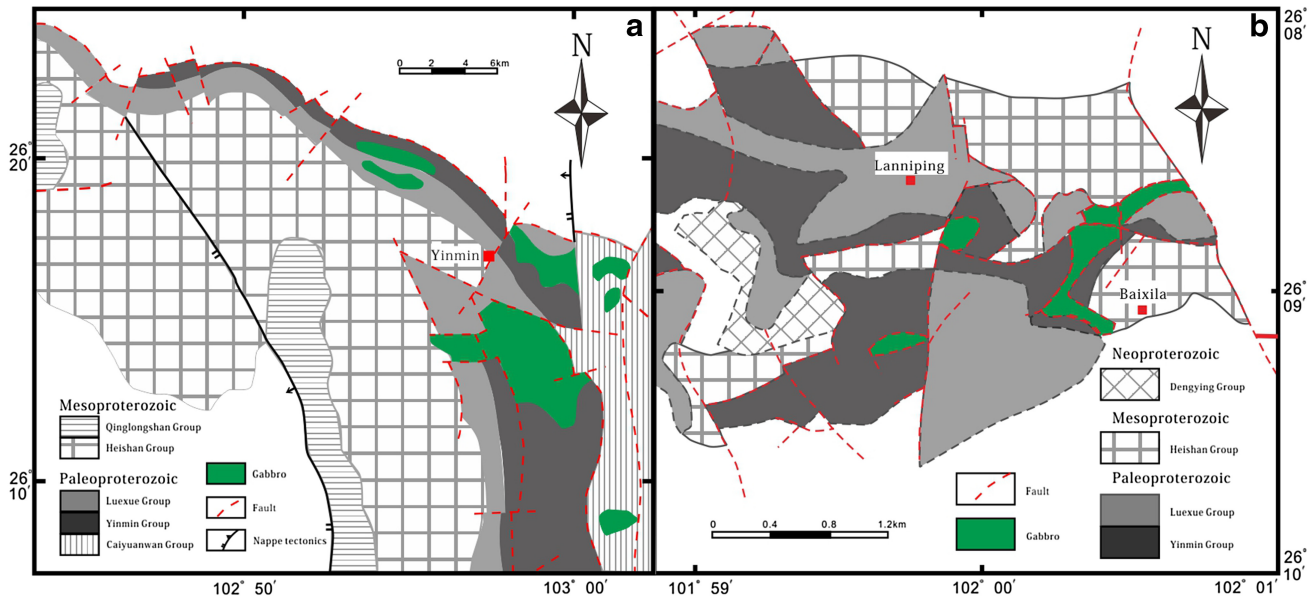

Fig. 2 Simplified geological map showing the distribution of gabbro intrusions and Proterozoic stratums in the Yinmin distinct (**a** Hou 2013) and Lanniping distinct (**b** Liu et al. 2012)

were altered to zoisite and hornblende. The dominant crystallization order for the gabbroic rocks is: plagioclase → clinopyroxene → magnetite and ilmenite. The gabbroic texture in the Lanniping intrusion is more distinct than in the Yinmin dykes. The Yinmin gabbroic dykes consist of approximately 40 vol% plagioclase, 40 vol% clinopyroxene, 5 vol%–10 vol% magnetite and minor ilmenite, hornblende, and biotite. In contrast, the Lanniping gabbroic intrusion contain 50 vol% plagioclase, 30 vol% clinopyroxene, 5 vol%–10 vol% ilmenite and minor magnetite, sulfides, apatite and hornblende.

In this study, thirty gabbroic rock samples were collected in the Yinmin and Lanniping areas around the Cu–Fe ore deposits. Fifteen samples were collected from open pits and surface outcrop in the Yinmin area, and all of them are hosted in the Yinmin or Luoxue Formations. Another fifteen samples were collected within the Lanniping intrusion. Three samples (YT-1-1, YT-1-4, YT-1-10) were collected under 3 mines, which were crossed by the gabbroic intrusion, and the other twelve samples were collected from the outcropped gabbroic intrusion. The Lanniping samples are also mainly hosted in the Lower Kunyang group (Fig. 2).

3 Sampling and analytical methods

Major elements of whole rocks were determined at the ALS laboratory by using ME-XRF 06 with <5 % relative standard deviation. Trace elements of whole rocks were analyzed by using inductively coupled plasma mass spectrometry (ICP-MS) at the State Key Laboratory of Ore Deposit Geochemistry, Chinese Academy of Sciences (SKLODG) with an analytical precision better than 5 %. The detailed procedure is similar to those described by Qi et al. (2000). The platinum-group elements were determined by isotope dilution (ID)-ICP-MS (Perkin-Elmer Sciex ELAN DRC-e) using a PTFE-lined, stainless steel pressure bomb technique (Qi et al. 2011). The mono-isotope element Rh was measured with external calibration using a ^{194}Pt spike as the internal standard (Qi et al. 2004). Ten grams of rock powder and an appropriate amount of enriched isotope spike solution containing ^{193}Ir, ^{101}Ru, ^{194}Pt, and ^{105}Pd were digested using ~5 ml of HF and ~15 ml of HNO_3 in a 120 ml PTFE beaker placed in a sealed, custom-made, high pressure, stainless steel (Qi et al. 2011). Total procedural blanks were lower than 0.002 ppb for Ir and Rh; 0.012 ppb for Ru; 0.040 ppb for Pd; and 0.002 ppb for Pt. As shown in Table 1, the results of the standard reference material WGB-1 (gabbro) agree well with the values reported by Qi et al. (2008). The accuracies are estimated to be better than 10 % for all PGEs. Sulfur contents were determined by a C–S analyzer at the SKLODG.

4 Analytical results

Concentrations and variations of PGE and S in the studied samples are listed in Tables 2 and 3, of which could be divided into two groups with high and low PGE contents for the Yinmin and Lanniping samples. The high PGE contents of the Yinmin samples (except samples YM1401 and YM1402) are in the same range as the high PGE contents of the Lanniping gabbroic rocks (LNP1217, LNP1229 and LNP1230). The samples with low PGE concentrations in the two districts share similar geochemical characteristics. However, most Yinmin samples have high PGE contents (PGEs = 13.9–87.0 ppb) and a majority of the Lanniping samples contain low PGE contents (PGEs = 0.12–1.02 ppb) could represent two groups considering the PGE concentrations. The samples with high PGE contents have relatively higher Ir (0.04–0.56 ppb), Ru (0.04–0.52 ppb), Rh (0.80–2.01 ppb), Pt (5.07–27.3 ppb), Pd (4.83–69.1 ppb) than the rocks with low PGE contents of Ir (<0.02 ppb), Ru (<0.02 ppb), Rh (<0.01 ppb), Pt (0.02–0.19 ppb), Pd (0.05–0.91 ppb) (Figs. 3, 5, 7). In contrast, the sulfur contents of the high-PGE samples (0.003–0.020 %) are lower than those of the low-PGE rocks (0.13–0.36 %). The Pt/Pd ratios of the high-PGE and low-PGE samples vary from ~0.64 and ~0.24. The Pd/Ir ratios in the high-PGE samples (55.2–712) are generally one order of magnitude higher than those of the low-PGE samples (3–395). Moreover, the PPGE concentrations in the high-PGE samples are much greater than those of the IPGE concentrations (Fig. 3). The high-PGE samples are characterized by lower and variable Cu/Pd ratios (2.8×10^2 to 3.5×10^4), which are much lower than those of the low-PGE samples (3.8×10^4 to 3.2×10^6).

There are positive correlations between MgO, Cr and Ru for the high-PGE samples, whereas MgO and Cr show poor relationships with Ru for the low-PGE rocks (Fig. 4). Binary variation diagrams of the PGE elements show poor relationships, except Pt vs. Pd for all samples (Fig. 5). The plots of S versus Ir, Rh, Pd, and Pt exhibit negative correlations for the high-PGE samples. However, there are no correlations between S and Ru for the high-PGE samples, or between S and PGEs for the low-PGE rocks (Fig. 7). There is a positive correlation between copper and sulfur in the high-PGE rocks, which is more obvious than between the low-PGE samples. There is a negative correlation between Pd and Cu/Pd (Fig. 6), and most of the high-PGE samples fall into the mantle; the enriched mantle areas indicate that the samples are rich in PGEs. In contrast, most of the low-PGE rocks fell into the depleted area due to their low PGE contents. The high-PGE group shared similar primitive mantle-normalized PGE patterns with the low-PGE group. The high-PGE samples were depleted in Ru

Table 1 Blank and detection limits (DL) of PGE (in ppb) for reference material WGB-1

Elements	Blank		WGB-1			
	Measured	DL	Measured	Qi et al. (2008)	Meisel and Moser (2004)	Certified
Ir	0.0017	0.001	0.16	0.16 ± 0.02	0.21	0.33
Ru	0.0124	0.001	0.12	0.13 ± 0.01	0.14	0.30
Rh	0.0019	0.001	0.22	0.20 ± 0.02	0.23	0.32
Pt	0.0015	0.009	5.39	6.34 ± 0.61	6.39	6.10
Pd	0.0396	0.015	13.84	13.0 ± 1.1	13.90	13.90

Certified Govindaraju (1994)

relative to Ir and Rh, and showed enrichment of PPGE relative to IPGE, whereas most samples were significantly richer in PPGEs compared to the primitive mantle (Barnes and Maier 1999). Rocks of low PGE contents are distinctly depleted compared to the primitive mantle (Fig. 3).

5 Discussion

5.1 Controls on PGE fractionation

Most studies have shown that the PGEs are relatively immobile during seafloor hydrothermal alteration (e.g., Rowell and Edgar 1986; Crocket 1990), but their immobility has been debated. For example, hydrothermal PGE mineralization has been proposed for the Cu-Ni sulfides at Rathbun Lake, northeastern Ontario (Rowell and Edgar 1986) and for the New Rambler mine in Wyoming (McCallum et al. 1976). Palladium has been found to be more mobile than Pt during different types of syn- to post-magmatic hydrothermal alteration (e.g., Li and Naldrett 1993), lower temperature alteration and serpentinization (e.g., Prichard et al. 2001; Seabrook et al. 2004) and weathering (e.g., Fuchs and Rose 1974; Prichard and Lord 1994). The relatively constant Ir and Ru concentrations for the two types of samples, and the positive correlation between Pt and Pd indicate that the original PGEs in the two study areas were not been affected by alteration (Figs. 3, 5).

Experiments have confirmed that there is only a slight difference in the partition coefficients of individual PGEs between sulfide and silicate melts (Naldrett and Duke 1980; Bezmen et al. 1994; Peach et al. 1994; Fleet et al. 1996). For example, partition coefficients of Ir and Pd between the sulfide melt and silicate melt are $(1.2–1.6) \times 10^4$ and 3.5×10^4, respectively (Peach et al. 1990). Bezmen et al. (1994), and the experimentally determined partition coefficients for Pd, Rh and Ir are: Pd $(5.5 \pm 0.7) \times 10^4$, Rh $(2.7 \pm 0.6) \times 10^4$ and Ir $(3.1 \pm 0.8) \times 10^4$. All these results show that there is little difference in the partition coefficients of IPGE and PPGE between the sulfide and the silicate melts. The high-PGE gabbroic samples exhibit four orders of magnitude higher PPGE contents relative to the IPGE contents, whereas the low-PGE samples are one order of magnitude for the PPGE to IPGE ratios, indicating different fractionation trends in the two groups (Table 2, 3). Thus, segregation of sulfides and the different degree of partial melting cannot explain the steeply positively-sloped primitive mantle-normalized patterns and the negative Ru anomalies of the samples. Crystal fractionation is considered important to the PPGE/IPGE ratios.

Barnes et al. (1985) showed that the high PPGE/IPGE ratio (e.g., Pd/Ir) might be caused by residual Os–Ir alloys during early mantle melting. In addition, IPGEs may form Os–Ir–Ru alloys during the early stages of crystal fractionation (Capobianco and Drake 1990; Amossé et al. 1990), which can be enclosed in the early phases (Stockman and Hlava 1984; Zhou 1994), effectively removing the IPGEs from the melt. Thus, the precipitation of IPGE-hosting alloys can also produce strong fractionation between the PPGEs and IPGEs. Negative Ru anomalies are generally attributed to the removal of Os–Ir–Ru alloys, together with chromite or olivine, from the parental magmas. Thus, it is suggested that the early removal of Os–Ir–Ru alloys could be one reason for the negative Ru anomalies and high PPGE/IPGE ratio in our samples. Moreover, the effect of the removal of Os–Ir–Ru alloys would be diluted by the segregation of sulfide phases for the low-PGE samples. As a result, the PPGE to IPGE ratios are not prominent, as PPGE contents are one order of magnitude higher than IPGE contents.

Righter et al. (2004) showed that spinel is particularly high in IPGEs, with the Ir and Pd partition coefficients in the range of 5–22,000 and 0.14. However, the Ir and Pd partition coefficients are 0.77 and 0.03, respectively, in olivine (Malvin et al. 1986; Ely and Neal 2003), 1.8 and 0.3, respectively, in clinopyroxene and 1.8 and 0.3, respectively, in orthopyroxene (Puchtel and Humayun 2001; Ely and Neal 2003). Thus, the fractionation of olivine, pyroxene could not significantly influence the PGE distributions in these rocks, except spinel. The IPGEs

Table 2 PGE (ppb), Cr, Ni, Cu, Zr, Hf (ppm) and MgO, S (%) concentrations of the Yinmin mafic dykes

Sample	Dykes														
	YM-16	YM-17	YM-18	YM-19	YM-20	YM-21	YM-22	YM-31	YM-1401	YM-1402	YM-35	YM-37	YM-40	YM-1403	YM-1404
Ir	0.23	0.25	0.24	0.15	0.29	0.16	0.13	0.08	0.02	0.01	0.04	0.20	0.56	0.13	0.19
Ru	0.24	0.39	0.44	0.52	0.12	0.04	0.04	0.22	0.01	0.01	0.24	0.14	0.46	0.30	0.25
Rh	1.05	0.96	1.39	1.17	2.01	1.38	1.52	1.27	0.003	0.02	1.07	1.06	1.56	0.74	0.80
Pt	15.3	13.1	10.9	10.8	27.3	42.7	16.3	7.45	0.11	0.12	5.07	14.4	14.3	16.0	16.5
Pd	21.9	30.6	13.0	32.8	41.8	38.6	69.1	4.83	0.17	0.21	30.8	20.8	21.5	36.5	32.2
PGE	38.7	45.3	26.0	45.4	71.5	82.9	87.0	13.9	0.31	0.37	37.2	36.6	38.3	53.6	49.9
S	0.013	0.010	0.014	0.012	0.004	0.003	0.006	0.014	0.114	0.257	0.009	0.005	0.009	0.020	0.010
Cr	106	120	106	177	60.3	20.5	22.1	51.7	182	133	72.6	95.9	115	118	110
Ni	112	81.7	100	104	37.4	28.0	29.7	55.1	33.1	26.2	60.0	36.1	74.9	92.6	87.3
Cu	129	950	125	1160	18.0	18.1	19.3	41.1	24.6	16.0	383	9.24	188	152	45.8
MgO	7.95	6.99	7.61	7.58	4.69	4.15	4.70	5.80	6.23	5.90	6.27	6.33	6.83	6.79	6.39
Pd/Ir	93.9	123	55.2	214	144	235	542	59.0	7.49	17.2	712	104	38.2	276	170
Pt/Pd	0.70	0.43	0.84	0.33	0.65	1.10	0.24	1.54	0.65	0.60	0.16	0.69	0.67	0.44	0.51
Cu/Pd	5.9×10^3	3.1×10^4	9.6×10^3	3.5×10^4	4.3×10^2	4.7×10^2	2.8×10^2	8.5×10^3	1.5×10^5	7.8×10^4	1.2×10^4	4.4×10^2	8.7×10^3	4.2×10^3	1.4×10^3

Table 3 PGE (ppb), Cr, Ni, Cu, Zr, Hf (ppm) and MgO, S (%) concentrations of the Lanniping mafic intrusions

Sample	Intrusions														
	LNP-1217	LNP-1224	LNP-1225	LN-P1226	LNP-1228	LNP-1229	LNP-1230	LNP1231	LNP1233	LNP-1401	LNP-1406	LNP-1407	YT-1-1	YT-1-4	YT-1-10
Ir	0.37	0.01	0.02	0.01	0.00	0.34	0.26	0.002	0.002	0.01	0.01	0.01	0.01	0.01	0.02
Ru	0.13	0.00	0.01	0.01	0.01	0.12	0.10	0.01	0.01	0.01	0.01	0.02	0.01	0.01	0.01
Rh	0.73	0.002	0.003	0.004	0.003	0.464	0.400	0.002	0.004	0.004	0.004	0.005	0.008	0.006	0.006
Pt	15.3	0.06	0.03	0.10	0.06	12.4	10.5	0.03	0.02	0.08	0.05	0.11	0.19	0.07	0.08
Pd	18.3	0.22	0.05	0.48	0.10	5.14	4.97	0.62	0.23	0.49	0.50	0.42	0.62	0.80	0.91
PGE	34.8	0.30	0.12	0.60	0.18	18.5	16.3	0.66	0.26	0.59	0.59	0.56	0.84	0.89	1.02
S	0.014	0.152	0.140	0.164	0.192	0.050	0.070	0.136	0.244	0.130	0.150	0.220	0.130	0.360	0.360
Cr	148	218	134	75.4	123	195	194	113	146	17.1	186	157	143	60.3	200
Ni	72.6	40.3	23.1	20.6	24.7	69.0	63.0	22.0	41.2	7.4	31.9	30.3	27.7	25.6	60.8
Cu	72.0	155	110	98.2	105	186	491	362	738	18.6	38.5	59.1	105	549	2440
MgO	6.20	8.38	5.87	5.26	5.62	5.88	5.59	5.40	8.47	3.12	6.02	5.77	5.23	5.09	9.26
Pd/Ir	55.0	24.8	2.66	62.7	26.2	15.1	18.8	395	140	69.3	33.6	58.4	96.5	82.1	39.2
Pt/Pd	0.85	0.28	0.63	0.20	0.59	2.42	2.12	0.05	0.09	0.16	0.11	0.26	0.31	0.09	0.09
Cu/Pd	3.5×10^3	7.0×10^5	2.1×10^6	2.0×10^5	1.1×10^6	3.6×10^4	9.9×10^4	5.9×10^5	3.2×10^6	3.8×10^4	7.7×10^4	1.4×10^5	1.7×10^5	6.9×10^5	2.7×10^6

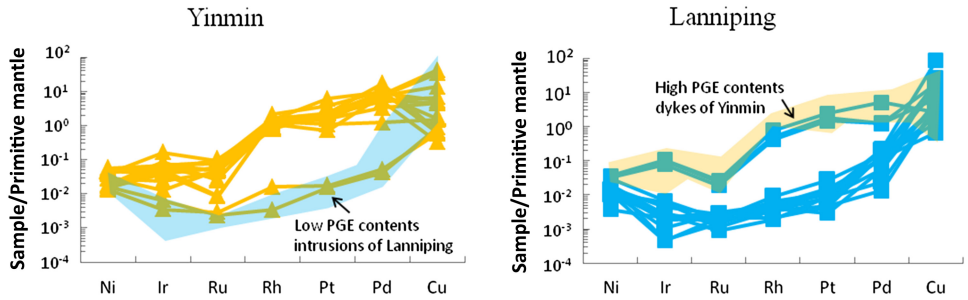

Fig. 3 Primitive mantle-normalized Cu, Ni, and PGE patterns for gabbrooic rocks from the Lanniping and Yinmin distincts of the Dongchuan area [normalization factors from Taylor and McLennan (1985)]

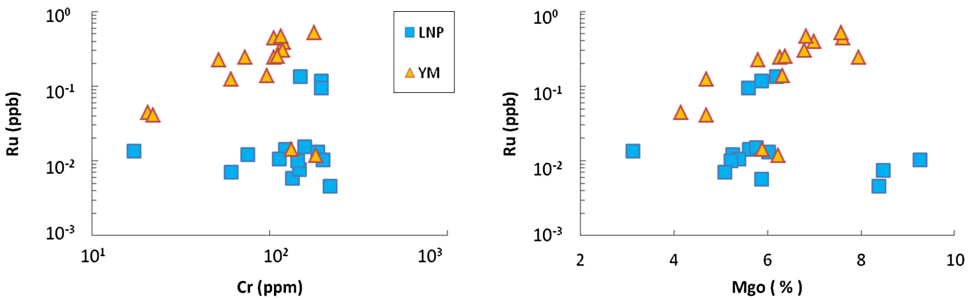

Fig. 4 Plots of Cr versus Ru, and MgO versus Ru contents in gabbroic rocks from the Dongchuan area

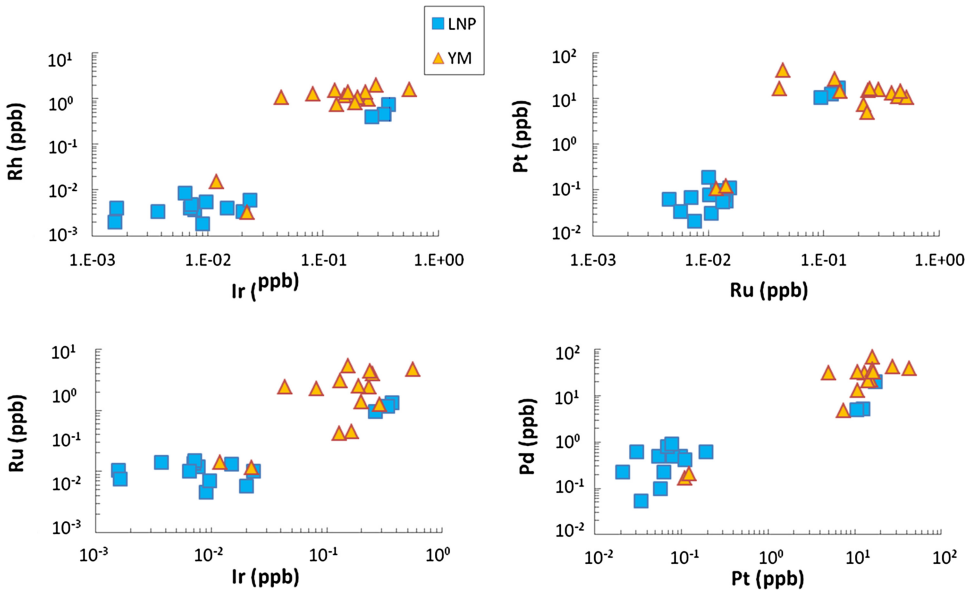

Fig. 5 Binary variation diagram for selected PGE in gabbroic rocks from the Dongchuan area

behave as compatible elements in many mafic magma systems and it is commonly suggested that they partition into spinel (e.g., Capobianco et al. 1994; Righter 2001). In contrast, Pt and Pd are incompatible in the spinel structure and their abundances increase in the fractionated magma during spinel crystallization. The solubility of IPGE in silicate magma is reduced significantly when the oxygen fugacity (fO_2) increases due to chromite precipitation (Amossé et al. 2000). For the high-PGE samples, PGEs are positively correlated with Cr (Fig. 4), showing that these elements are likely mainly controlled by chromite/spinel during crystal fractionation. The plot of Ni/Cu to Pd/Ir indicates the spinel trend for the high-PGE samples (Fig. 8). In addition, Capobianco and Drake (1990) found that Ru was strongly partitioned into spinel (D = 22–25). Moreover, early higher-temperature spinel condensates are likely to be enriched in Ru over Ir (Righter and Downs 2001). For the low-PGE samples, few of the chromite/spinel left the residual parental magma, as PGEs are not correlated with Cr (Fig. 4). Therefore, the fractionation and removal of chromite/spinel from parental magma during ascent could also be responsible for the negative Ru

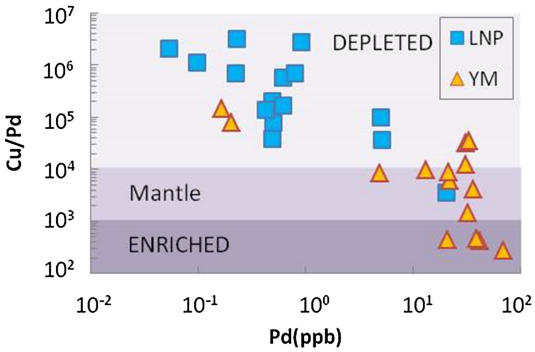

Fig. 6 Plot of Cu/Pd versus Pd showing the composition of the gabbroic rocks from different distincts of the Dongchuan area (fields from Barnes et al. 1993)

anomalies and high PPGE/IPGE ratio for the high-PGE samples. The Ni contents are lower than the Cu contents for all samples (Fig. 3), which could be caused by the removal of olivine, due to the compatibility of Ni in olivine.

5.2 Sulfide segregation

Chalcophile elements such as Ni, Cu and PGE strongly partition into sulfide liquid due to the high partition coefficients between sulfide and silicate liquids (10^4–10^5 for PGE: Stone et al. 1990; Bezmen et al. 1994; Peach et al. 1994; Fleet et al. 1996; Crocket and Fleet 1997 or $\sim 10^7$–10^{11} for PGE: Fonseca et al. 2009; 10^2–10^3 for Cu and Ni: Rajamani and Naldrett 1978; Francis 1990; Peach et al. 1990; Gaetani and Grove 1997). The distribution of the platinum element and copper in mafic and ultramafic rocks is therefore controlled by magmatic sulfides, PGMs (platinum-group minerals) and, to a lesser extent, oxides (chromite) and silicates (olivines; e.g., Barnes et al. 1985). In the upper mantle, sulfide is usually distributed in the surrounding of mineral particles as a function of the segregation of sulfides (Mitchell and Keays 1981). The segregation of sulfides may result in the depletion of PGE and other metallic elements in the evolved magma (Naldrett

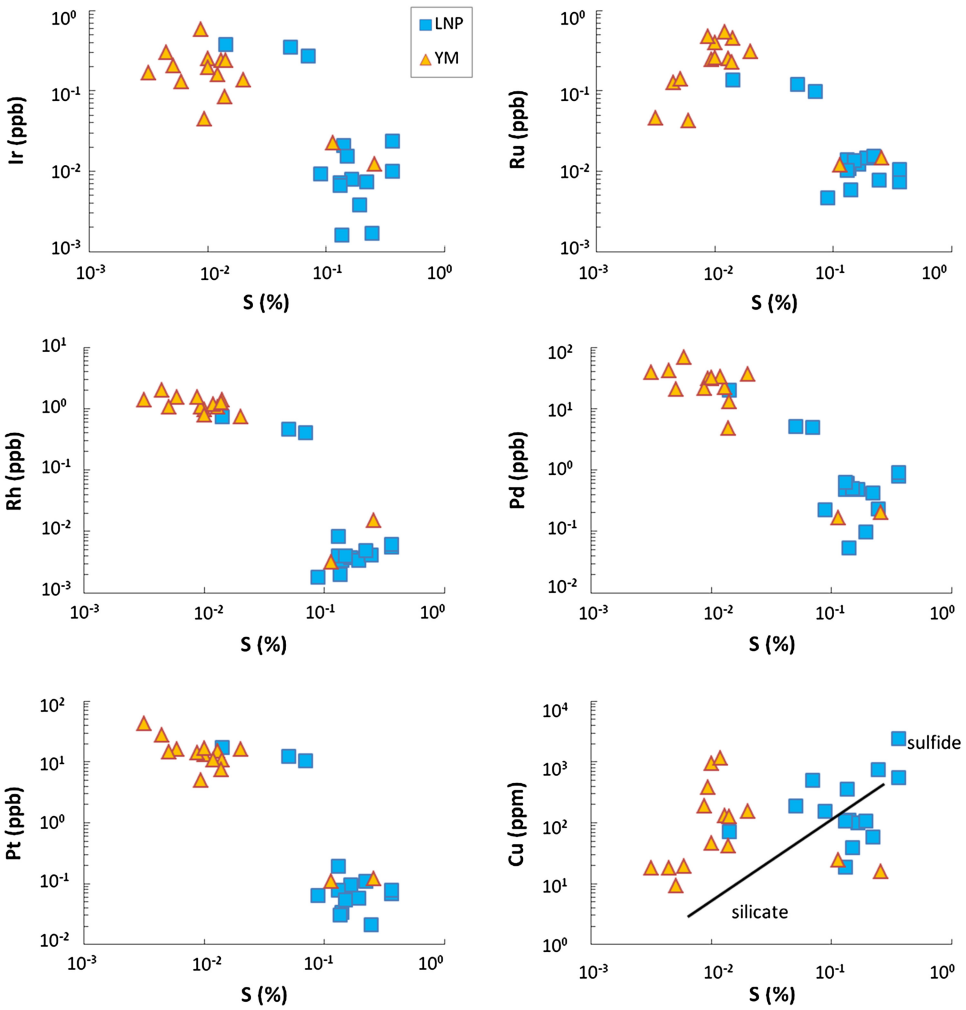

Fig. 7 Plots of S versus Ir, Ru, Rh, Pd, Pt and Cu for the Lanniping gabbroic intrusion and Yinmin mafic dykes at Dongchuan

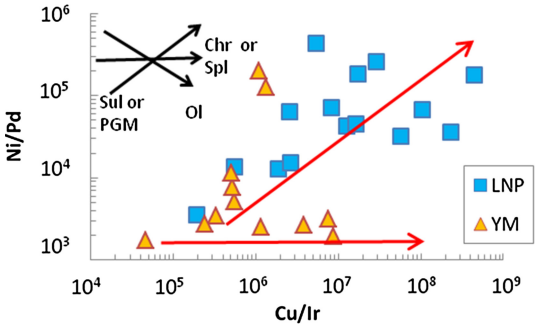

Fig. 8 Plot of Ni/Pd versus Cu/Ir for the Lanniping gabbroic intrusion and Yinmin mafic dykes at Dongchuan. The direction of the arrow indicates the differentiation trend of minerals in the figure (Barnes et al. 1988). Chr chromite, Ol olivine, Sul or PGM sulfide and PGM

and Wilson 1990). The segregation of sulfides from crystallizing silicate magma is considered to be crucial in the formation of PGE (Keays 1995). If rocks contain magmatic sulfides, the PGE concentrations of rocks will be mostly controlled by sulfide. The inference of the partition coefficients for PGEs between the sulfide and silicate magma were much higher than copper and nickel as shown in the plot of Cu/Ir vs. Ni/Pd diagram (Fig. 8). The high Ni/Pd and Cu/Ir ratios of the low-PGE samples suggest that the magma may have experienced a segregation of minor sulfides before emplacement. In contrast, the effect of sulfide segregation does not occur for the initial S-unsaturated magmas with high-PGE contents.

Mafic rocks containing >1000 ppm S are considered to be sulfide saturated (Hoatson and Keays 1989). The low-PGE samples have high S contents (1140–3600 ppm), indicating that they reached sulfur saturation. In contrast, the high-PGE samples have low S contents (30–140 ppm), much lower than 1000 ppm (Tables 2, 3), suggesting they did not achieve sulfur saturation. The Cu/Pd ratio is a sensitive indicator for sulfide segregation and is useful in local or regional Ni, Cu and PGE exploration (Barnes et al. 1985). Most of the low-PGE samples have Cu/Pd ratios higher than that of the mantle (Cu/Pd = 1000–10,000) and are depleted in palladium to copper, as shown in the Cu/Pd versus palladium diagram (Fig. 6). This feature suggests that these rocks may have experienced sulfide segregation prior to their final emplacement. Sulfide is the main control on PGE concentrations factor for S-saturated melts. Therefore, there is a potential for finding PGE-rich mineralization close to or within the gabbroic intrusion in the Lanniping area.

In order to examine the extent of the sulfide segregation, we model the degree of sulfide segregation to produce the low-PGE rocks. The amount of segregated sulfides may be estimated from the following mass balance equation (Barnes et al. 1993):

Table 4 Percentage of sulfide segregation for the low-PGE samples from Yinmin and Lanniping

X	Ir (ppb)	Ru (ppb)	Rh (ppb)	Pt (ppb)	Pd (ppb)
0.005 %	0.11	0.56	0.77	0.17	0.18
0.01 %	0.06	0.28	0.39	0.09	0.09
0.05 %	0.01	0.06	0.08	0.02	0.02
0.1 %	0.01	0.03	0.04	0.01	0.01
0.5 %	0.00	0.01	0.01	0.00	0.00
Mantle	4.4	5.6	1.6	8.3	4.4

Barnes et al. 1988

$$C_F/C_L = 1/[1 + X(D - 1)/100]$$

where C_F = the concentration of the element in the fractionated in the initial magma: Ir = 4.4 ppb, Ru = 5.6 ppb, Rh = 1.6 ppb, Pt = 8.3 ppb, Pd = 4.4 ppb (Barnes et al. 1988); C_L = the concentration of the element in the initial magma; D = the partition coefficient of the element between the sulfide and the silicate: $D(Ir) = 51 \times 10^3$, $D(Ru) = 7 \times 10^3$, $D(Pt) = 16.5 \times 10^3$, $D(Pd) = 28 \times 10^3$ (Crocket and Fleet 1997), $D(Rh) = 27 \times 10^3$ (Bezmen et al. 1991); and X = the weight percent sulfide that segregated. The calculation shows that 0.01 %–0.1 % sulfides have been removed from the magma in the magma chamber (Table 4). As shown in the diagram, 0.1 % sulfides segregation would lead to very low PGE in the magma.

5.3 Implications for mantle source, magma evolution and sulfide segregation

It has been suggested that the Yinmin mafic dykes and Lanniping gabbroic intrusions were generated from similar tectonic environments (Greentree et al. 2006, 2008; Zhao et al. 2010). As shown above, the mafic rocks from different areas share similar compositional ranges of PGE concentrations, although most of the Yinmin gabbroic dykes contain relatively high PGE contents, and most of the Lanniping gabbroic intrusive samples have low PGE contents and small amounts of sulfides. The evolution of magmas generating the mafic rocks could be inferred from the features of PGE and S, MgO, Cr concentrations (Barnes et al. 1985, 1988; Naldrett and Wilson 1990; Naldrett 2010), indicating that they were possibly subjected to the removal of chromite/spinel, olivine and Os–Ir–Ru alloys before deposition and sulfide segregation.

For the partial melting in the mantle, the chalcophile elements enter the melt at different rates, depending on the degree of melting. However, once there is sufficient magma to dissolve the entire sulfide, they reach their maximum concentrations, and subsequently are diluted

with further melting as the mass of magma increases without the addition of PGE and Cu (Wendlandt 1982; Hart and Zindler 1986; Mavrogenes and O'Neill 1999; Ghiorso et al. 2002). Naldrett (2010) inferred that all sulfides in the mantle are dissolved into the melt and leave their source when magma is produced by 18 % partial melting, and thus Cu, Pt and Pd are at their maxima. The supposed maximum Pt and Pd contents both are 18 ppb. However, the sum of the Pt and Pd contents (23.5–85.3 ppb) for the high-PGE samples in Yinmin are higher than 36 ppb and their S contents are much lower than 1000 ppm, indicating that the degrees of partial melting are lower than 18 % and their parental magmas are S-undersaturated. As a result, their Pt and Pd concentrations increased with the evolution of the initial S-unsaturated magmas. In contrast, the parental magmas generating the low-PGE samples were subjected to sulfide saturation and lost small amounts of PGE-bearing sulfides.

As demonstrated above, during the ascent of the parental magma, possible removal of Os–Ir–Ru and/or chromite/spinel for the Yinmin high-PGE samples results in high Pd/Ir ratios and Ru anomalies. In the same way, the Lanniping low-PGE samples exhibit relatively lower Pd/Ir ratios and Ru anomalies. It has been suggested that the parental magmas of the Yinmin gabbroic dykes were originally S-undersaturated, as shown from high PGE and low S contents in most samples. Subsequently, minor evolved magma reached sulfur saturation and resulted in sulfide segregation, generating two PGE-depleted and high-S samples. In contrast, during the evolution of parental magma, the segregation of sulfide may result in the low PGE contents for the Lanniping low-PGE samples. The high Cu/Pd ratios also support the characteristic of S-saturated or sulfide segregation for the low-PGE rocks. The initial stage of the Lanniping parental magma is S-unsaturated, as shown from the three samples with high PGE concentrations and low S contents. In this regard, the segregated sulfides enriched in PGE could stay somewhere close to or within the Lanniping intrusion, providing a possible opportunity to discover the PGE-enriched sulfide mineralization.

6 Summary

(i) The Yinmin mafic dykes and Lanniping gabbroic intrusion share the same compositional ranges of PGE concentrations. However, most of the Yinmin gabbroic dykes contain relatively high PGE concentrations and low S contents, and most of the Lanniping samples have low PGE concentrations and elevated S contents.

(ii) During ascent of the parental magma, removal of Os–Ir–Ru and/or the chromite/spinel result in high Pd/Ir ratios and Ru anomalies for the Yinmin high-PGE samples and relatively lower Pd/Ir ratios and Ru anomalies for the Lanniping low-PGE samples. It has been demonstrated that the parental magmas of the Yinmin gabbroic dykes were initially S-undersaturated, and subsequently, minor evolved magma reached sulfur saturation which resulted in sulfide segregation.

(iii) Sulfide segregation is the major control on the PGE-poor melts. Most Lanniping samples have higher Cu/Pd ratios, suggesting that these rocks may have experienced sulfide segregation. The calculation indicated that 0.01 %–0.1 % sulfide had been removed from the melts due to S-oversaturation, therefore generating the PGE-depleted Lanniping samples. Thus, the potential exists to discover PGE-enriched sulfide mineralization somewhere close to or within the Lanniping mafic intrusion.

Acknowledgments We appreciate the assistance of Prof. Liang Qi and Ms. Yan Huang in the trace element and PGE analyses. The constructive comments and suggestions of the reviewers are acknowledged. This study was supported by the National Natural Science Foundation of China (41425011 and 41303016).

References

Amossé J, Dable P, Allibert M (2000) Thermochemical behaviour of Pt, Ir, Rh and Ru vs fO_2 and fS_2 in a basaltic melt. Implications for the differentiation and precipitation of these elements. Miner Petrol 68(1–3):29–62

Amossé J, Allibert M, Fischer W, Piboule M (1990) Experimental study of the solubility of platinum and iridium in basic silicate melts—implications for the differentiation of platinum-group elements during magmatic processes. Chem Geol 81(1):45–53

Barnes SJ, Maier W (1999) The fractionation of Ni, Cu and the noble metals in silicate and sulphide liquids. Geol Assoc Can Short Course Notes 13:69–106

Barnes SJ, Naldrett A, Gorton M (1985) The origin of the fractionation of platinum-group elements in terrestrial magmas. Chem Geol 53(3):303–323

Barnes SJ, Boyd R, Korneliussen A, Nilsson L, Often M, Pedersen R, Robins B (1988) The use of mantle normalization and metal ratios in discriminating between the effects of partial melting, crystal fractionation and sulphide segregation on platinum-group elements, gold, nickel and copper: examples from Norway Geoplatinum, vol 87. Springer, Berlin, pp 113–143

Barnes SJ, Couture J, Sawyer E, Bouchaib C (1993) Nickel-copper occurrences in the Belleterre-Angliers Belt of the Pontiac Subprovince and the use of Cu-Pd ratios in interpreting platinum-group element distributions. Econ Geol 88(6):1402–1418

Bezmen N, Brügmann GY, Naldrett A (1991) Mechanism of concentration of platinum-group elements: partitioning between silicate and sulfide melts. Int Geol Rev 33(8):784–792

Bezmen N, Asif M, Brügmann G, Romanenko I, Naldrett A (1994) Distribution of Pd, Rh, Ru, Jr, Os, and Au between sulfide and silicate metals. Geochim Cosmochim Acta 58(4):1251–1260

Capobianco CJ, Drake MJ (1990) Partitioning of ruthenium, rhodium, and palladium between spinel and silicate melt and implications for platinum group element fractionation trends. Geochim Cosmochim Acta 54(3):869–874

Capobianco CJ, Hervig RL, Drake MJ (1994) Experiments on crystal/liquid partitioning of Ru, Rh and Pd for magnetite and hematite solid solutions crystallized from silicate melt. Chem Geol 113(1):23–43

Chen G (1998) Geologic eatures of the gabbro type Cu deposit in Dongchuan and their ore-prospecting significance. Geol Yunnan 01:78–83

Crocket JH (1990) Noble metals in seafloor hydrothermal mineralization from the Juan de Fuca and mid-Atlantic ridges: a fractionation of gold from platinum metals in hydrothermal fluids. Can Miner 28:639–648

Crocket J, Fleet M (1997) Implications of composition for experimental partitioning of platinum-group elements and gold between sulfide liquid and basalt melt: the significance of nickel content. Geochim Cosmochim Acta 61(19):4139–4149

Ely JC, Neal CR (2003) Using platinum-group elements to investigate the origin of the Ontong Java Plateau, SW Pacific. Chem Geol 196(1):235–257

Fleet M, Crocket J, Stone W (1996) Partitioning of platinum-group elements (Os, Ir, Ru, Pt, Pd) and gold between sulfide liquid and basalt melt. Geochim Cosmochim Acta 60(13):2397–2412

Fonseca RO, Campbell IH, O'Neill HSC, Allen CM (2009) Solubility of Pt in sulphide mattes: implications for the genesis of PGE-rich horizons in layered intrusions. Geochim Cosmochim Acta 73(19):5764–5777

Francis RD (1990) Sulfide globules in mid-ocean ridge basalts (MORB), and effect of oxygen abundance in Fe-S-O liquids on the ability of those liquids to partitionmetals fromMORB and komatiitemagmas. Chem Geol 85:199–213

Fuchs WA, Rose AW (1974) The geochemical behavior of platinum and palladium in the weathering cycle in the Stillwater Complex, Montana. Econ Geol 69:332–346

Gaetani GA, Grove TL (1997) Partitioning of moderately siderophile elements among olivine, silicate melt, and sulfide melt: constraints on core formation in the Earth and Mars. Geochim Cosmochim Acta 61(9):1829–1846

Geng Y, Yang C, Du L, Wang X, Ren L, Zhou X (2007) Chronology and tectonic environment of the Tianbaoshan Formation: new evidence from zircon SHRIMP U-Pb age and geochemistry. Geol Rev 53(4):556–563

Ghiorso MS, Hirschmann MM, Reiners PW, Kress VC (2002) The pMELTS: a revision of MELTS for improved calculation of phase relations and major element partitioning related to partial melting of the mantle to 3 GPa. Geochem Geophys Geosyst 3:1–35

Gong L, Wang C (1981) On the origin of "Dongchuan type" copper deposit: Scientia Geologica Sinica, pp 203–211 (in Chinese)

Gong L, He Y, Chen T (1996) Proterozoic Dongchuan-type rift Cudeposit in Yunnan. Metallurgical Industry Publication, Beijing (in Chinese)

Govindaraju K (1994) 1994 compilation of working values and sample description for 383 geostandards. Geostand Newslett 18(S1):1–158

Greentree MR, Li ZX (2008) The oldest known rocks in south-western China: SHRIMP U-Pb magmatic crystallisation age and detrital provenance analysis of the Paleoproterozoic Dahongshan Group. J Asian Earth Sci 33(5):289–302

Greentree MR, Li ZX, Li XH, Wu H (2006) Late Mesoproterozoic to earliest Neoproterozoic basin record of the Sibao orogenesis in western South China and relationship to the assembly of Rodinia. Precambr Res 151(1):79–100

Hamlyn PR, Keays RR, Cameron WE, Crawford AJ, Waldron HM (1985) Precious metals in magnesian low-Ti lavas: implications for metallogenesis and sulfur saturation in primary magmas. Geochim Cosmochim Acta 49(8):1797–1811

Hart SR, Zindler A (1986) In search of a bulk-Earth composition. Chem Geol 57:247–267

He D (2009) Petrological and geochemical characteristics of the Lala copper deposit in Sichuan Province. Unpublished Ph.D. thesis, The Gradute School of the Chinese Academy of Sciences, China, p 103

Hoatson DM, Keays RR (1989) Formation of platiniferous sulfide horizons by crystal fractionation and magma mixing in the Munni layered intrusion, West Pilbara Block, Western Australia. Econ Geol 84(7):1775–1804

Hou L (2013) Proterozoic Fe-Cu-Au-REE metallogenic system of "Dongchuan" Group in central Yunnan procince-A case study on the Ynachang deposit. Ph.D. Dissertation, China University of Geosciences

Hou L, Ding J, Deng J, Peng HJ (2015) Geology, geochronology, and geochemistry of the Yinachang Fe–Cu–Au–REE deposit of the Kangdian region of SW China: evidence for a Paleo-Mesoproterozoic tectono-magmatic event and associated IOCG systems in the western Yangtze Block. J Asian Earth Sci 103:129–149

Hua RM (1990) The sedimentation-reworking genesis of Dongchuan-type stratiform copper deposits. Chin J Geochem 9:231–243

Keays RR (1995) The role of komatiitic and picritic magmatism and S-saturation in the formation of ore deposits. Lithos 34(1):1–18

Li CS, Naldrett AJ (1993) High chlorine alteration minerals and calcium-rich brines in fluid inclusions from the Strathcona deep copper zone, Sudbury, Ontario. Econ Geol 88:1780–1796

Li XJ, Hua RY, Li LJ, Fan CY, Duan GL, Qu YC (1953) Geology of the Dongchuan-type copper deposit in Yunnan. Acta Geol Sinica 33:76–84 **(in Chinese)**

Li XH, Li ZX, Ge W, Zhou H, Li W, Liu Y, Wingate MTD (2003a) Neoproterozoic granitoids in South China: crustal melting above a mantleplume at ca. 825 Ma? Precambr Res 122:45–83

Li ZQ, Wang JZ, Liu JJ, Li CY, Du AD, Liu YP, Ye L (2003b) Re-Os dating of molydenite from Lala Fe-Oxide-Cu-Au-Mo-REE deposit, Southwest China: implications for ore genesis. Contrib Geol Miner Resour 18:39–42 **(in Chinese with English abstract)**

Li ZX, Wartho JA, Occhipinti S, Zhang CL, Li XH, Wang J, Bao C (2007) Early history of the eastern Sibao Orogen (South China) during the assembly of Rodinia: new mica 40Ar/39Ar dating and SHRIMP U-Pb detrital zircon provenance constraints. Precambr Res 159(1):79–94

Lightfoot PC, Keays RR (2005) Siderophile and chalcophile metal variations in flood basalts from the Siberian trap, Noril'sk region: implications for the origin of the Ni-Cu-PGE sulfide ores. Econ Geol 100(3):439–462

Liu YL, Fang WX, Pan HJ, Du YL, Yao F (2011) Geologic characteristics of gabbro-diorite rock mass of the Lanniping district of the Dongchuan copper deposits and their ore-prospecting significance. Miner Resour Geol 25(2):143–147 **(in Chinese with English abstract)**

Liu WM, Liu JS, Liu WH, Yang LG, Zhou YG, Dong X (2012) Ore geochemical characteristics and genesis of Xikuangshan type Fe-Cu deposit in Lanniping-Baixila copper mine of Dongchuan. World Geol 31(2):281–289 **(in Chinese with English abstract)**

Maier WD (2005) Platinum-group element (PGE) deposits and occurrences: mineralization styles, genetic concepts, and exploration criteria. J Afr Earth Sc 41(3):165–191

Malvin D, Drake M, Benjamin T, Duffy C, Hollander M, Rogers P (1986) Experimental partitioning studies of siderophile elements

amongst lithophile phases: preliminary results using PIXE microprobe analysis. In: Paper presented at the Lunar and Planetary Science Conference

Mavrogenes JA, O'Neill HSC (1999) The relative effects of pressure, temperature and oxygen fugacity on the solubility of sulfide in mafic magmas. Geochim Cosmochim Acta 63:1173–1180

McCallum M, Loucks R, Carlson R, Cooley E, Doerge T (1976) Platinum metals associated with hydrothermal copper ores of the New Rambler Mine, Medicine Bow Mountains, Wyoming. Econ Geol 71(7):1429–1450

Meisel T, Moser J (2004) Reference materials for geochemical PGE analysis: new analytical data for Ru, Rh, Pd, Os, Ir, Pt and Re by isotope dilution ICP-MS in 11 geological reference materials. Chem Geol 208(1):319–338

Meng HM, Chang HC, Hsu SC, Teng YS, Shu CA (1948) Geology of the Tungchuan district, northeastern Yunnan, vol 68. National Research Institute of Geology, Shanghai

Mitchell RH, Keays RR (1981) Abundance and distribution of gold, palladium and iridium in some spinel and garnet lherzolites: implications for the nature and origin of precious metal-rich intergranular components in the upper mantle. Geochim Cosmochim Acta 45(12):2425–2442

Mou C, Lin S, Yu Q (2003) The U-Pb ages of the volcanic rock of the Tianbaoshan formation, Huili, Sichuan province. J Stratigr 27:216–219

Naldrett AJ (2010) Secular variation of magmatic sulfide deposits and their source magmas. Econ Geol 105(3):669–688

Naldrett AJ, Duke JM (1980) Platinum metals magmatic sulfide ores. Science 208(4451):1417–1424

Naldrett AJ, Wilson AH (1990) Horizontal and vertical variations in noble-metal distribution in the Great Dyke of Zimbabwe: a model for the origin of the PGE mineralization by fractional segregation of sulfide. Chem Geol 88(3):279–300

Peach C, Mathez E, Keays R (1990) Sulfide melt-silicate melt distribution coefficients for noble metals and other chalcophile elements as deduced from MORB: implications for partial melting. Geochim Cosmochim Acta 54(12):3379–3389

Peach C, Mathez EA, Keays RR, Reeves S (1994) Experimentally determined sulfide melt-silicate melt partition coefficients for iridium and palladium. Chem Geol 117(1):361–377

Prichard H, Lord R (1994) Evidence for differential mobility of platinum-group elements in the secondary environment in Shetland ophiolite complex. Trans Inst Min Metall B 103:53–56

Prichard HM, Sá JHS, Fisher PC (2001) Platinum-group mineral assemblages and chromite composition in the altered and deformed Bacuri complex, Amapa, northeastern Brazil. Can Miner 39(2):377–396

Puchtel IS, Humayun M (2001) Platinum group element fractionation in a komatiitic basalt lava lake. Geochim Cosmochim Acta 65(17):2979–2993

Qi L, Zhou MF (2008) Platinum-group elemental and Sr–Nd–Os isotopic geochemistry of Permian Emeishan flood basalts in Guizhou Province, SW China. Chem Geol 248(1):83–103

Qi L, Jing H, Gregoire DC (2000) Determination of trace elements in granites by inductively coupled plasma mass spectrometry. Talanta 51(3):507–513

Qi L, Zhou MF, Wang CY (2004) Determination of low concentrations of platinum group elements in geological samples by ID-ICP-MS. J Anal At Spectrom 19(10):1335–1339

Qi L, Gao J, Huang X, Hu J, Zhou M-F, Zhong H (2011) An improved digestion technique for determination of platinum group elements in geological samples. J Anal Atom Spectrom 26(9):1900–1904

Qian J, Shen Y (1990) The Dahongshan volcanogenic Fe-Cu deposit in Yunnan Province. Geological Publishing House, Beijing

Qiu HN, Zhu BQ, Sun DZ (2002) Age significance interpreted from $^{40}Ar/^{39}Ar$ dating of quartz samples from the Dongchuan Copper Deposits, Yunnan, SW China, by crushing and heating. Geochem J. 36:475–491

Rajamani V, Naldrett AJ (1978) Partitioning of Fe Co, Ni, and Cu between sulfide liquid and basaltic melts and the composition of Ni-Cu sulfide deposits. Econ Geol 73(1):82–93

Ran CY (1983) On genetic model of Dongchuan type strata-bound copperdeposit. Scientia Sinica Ser B 26:983–993

Righter K (2001) Rhenium and iridium partitioning in silicate and magmatic spinels: implications for planetary magmatism and mantles. In: Paper presented at the Lunar and Planetary Science Conference

Righter K, Downs RT (2001) The crystal structures of synthetic Re- and PGE-bearing magnesioferrite spinels: implications for impacts, accretion and the mantle. Geophys Res Lett 28:619–622

Righter K, Campbell A, Humayun M, Hervig R (2004) Partitioning of Ru, Rh, Pd, Re, Ir, and Au between Cr-bearing spinel, olivine, pyroxene and silicate melts. Geochim Cosmochim Acta 68(4):867–880

Rowell WF, Edgar AD (1986) Platinum-group element mineralization in a hydrothermal Cu-Ni sulfide occurrence, Rathbun Lake, northeastern Ontario. Econ Geol 81(5):1272–1277

Seabrook CL, Prichard HM, Fisher PC (2004) Platinum-group minerals in the Raglan Ni–Cu–(PGE) sulfide deposit, Cape Smith, Quebec, Canada. Can Miner 42(2):485–497

Seitz HM, Keays RR (1997) Platinum group element segregation and mineralization in a noritic ring complex formed from Proterozoic siliceous high magnesium basalt magmas in the Vestfold Hills, Antarctica. J Petrol 38(6):703–725

Stockman HW, Hlava PF (1984) Platinum-group minerals in alpine chromitites from southwestern Oregon. Econ Geol 79(3):491–508

Stone W, Crocket J, Fleet M (1990) Partitioning of palladium, iridium, platinum, and gold between sulfide liquid and basalt melt at 1200 C. Geochim Cosmochim Acta 54(8):2341–2344

Sun K, Shen Y, Liu G, Li Z, Pan X (1991a) Proterozoic iron-copper deposits in central Yunnan province. China University of Geoscience Press, Beijing, pp 145–177

Sun SS, Wallace D, Hoatson D, Glikson A, Keays R (1991b) Use of geochemistry as a guide to platinum group element potential of mafic-ultramafic rocks: examples from the west Pilbara Block and Halls Creek Mobile Zone, Western Australia. Precambrian Res 50(1):1–35

Sun WH, Zhou MF, Gao JF, Yang YH, Zhao XF, Zhao JH (2009) Detrital zircon U-Pb geochronological and Lu–Hf isotopic constraints on the Precambrian magmatic and crustal evolution of the western Yangtze Block, SW China. Precambrian Res 172(1):99–126

Taylor SR, McLennan SM (1985) The continental crust: its composition and evolution. Blackwell, Oxford

Wendlandt RF (1982) Sulfide saturation of basalt and andesite melts at high pressures and temperatures. Am Mineral 67:877–885

Wu MD, Wang JS, Song XL, Chen L, Dan Y (1990) Geology of Kunyang Group in Yunnan Province. Scientific Press of Yunnan Province, Kunming **(in Chinese with English abstract)**

Ye L, Li CY, Liu JJ, Liu YP (2004) Ar-Ar isotope age of Yinachang copper deposit, Wuding, Yunnan Province, China and its implications. Acta Miner Sinica 24:411–414 **(in Chinese with English abstract)**

Yin F, Sun Z, Zhang Z (2011) Mesoproterozoic stratigraphic-structure framework in Huili-Dongchuan area. Geological Review 57:770–778

Zhang C, Gao L, Wu Z, Shi X, Yan Q, Li D (2007) SHRIMP U-Pb zircon age of tuff from the Kunyang Group in central Yunnan:

evidence for Grenvillian orogeny in South China. Chin Sci Bull 52(11):1517–1525

Zhao XF, Zhou MF (2011) Fe–Cu deposits in the Kangdian region, SW China: a Proterozoic IOCG (iron-oxide–copper–gold) metallogenic province. Miner Deposita 46(7):731–747

Zhao XF, Zhou MF, Li JW, Sun M, Gao JF, Sun WH, Yang JH (2010) Late Paleoproterozoic to early Mesoproterozoic Dongchuan Group in Yunnan, SW China: implications for tectonic evolution of the Yangtze Block. Precambr Res 182(1):57–69

Zhao JH, Zhou MF, Yan DP, Zheng JP, Li JW (2011) Reappraisal of the ages of Neoproterozoic strata in South China: no connection with the Grenvillian orogeny. Geology 39:299–302

Zhao XF, Zhou MF, Li JW, Qi L (2013) Late Paleoproterozoic sedimentary rock-hosted stratiform copper deposits in South China: their possible link to the supercontinent cycle. Miner Deposita 48(1):129–136

Zhou MF (1994) PGE distribution in 2.7-Ga layered komatiite flows from the Belingwe greenstone belt, Zimbabwe. Chem Geol 118(1):155–172